Doping-profile effects on the tunneling times of electrons confined in double-barrier heterostructures

N. Mingo, J. A. Porto, and J. Sánchez-Dehesa

Departamento de Física de la Materia Condensada, Facultad de Ciencias (C-XII), Universidad Autónoma de Madrid, E-28049 Madrid, Spain

(Received 27 May 1994)

We study and compare the behavior of the left- and right-tunneling times of electrons quasiconfined in asymmetric double-barrier structures as a function of the bias for two different doping configurations in the electrodes: uniform doping and gradual doping. The potential experienced by the electrons is calculated self-consistently for each case by simultaneously solving the Schrödinger and Poisson equations. Afterwards, the stabilization method is employed to calculate the corresponding tunneling times. The case of gradual doping is especially interesting because an accumulation layer appears when the voltage is high enough. To analyze the stabilization graphs in the range of voltages where the two-dimensional quasiconfined level in the emitter interacts with the quantum-well level we have introduced a three-level model. We present a comparison of the tunneling times calculated for the two doping profiles with the ones obtained with a model potential. Finally, charge-accumulation effects are analyzed in the gradually doped case and critically discussed within the framework of available experimental data.

I. INTRODUCTION

A great deal of work has been devoted in recent years to studying double-barrier resonant-tunneling structures (DBRTS's) in order to analyze different issues in quantum transport. One of the goals of such efforts is to understand the mechanisms responsible for the tunneling across the classically forbidden region. In that sense the first difficulty to overcome is to define a tunneling time. Hauge and Støvneng,[1] Jauho,[2] and Landauer and Martin[3] have reviewed the recent advances on that topic; in particular, they present the different tunneling times defined up to date and critically discuss them. The present work is devoted to studying the lifetime of electrons quasiconfined in DBRTS's. The tunneling time definition we work with is the well known decay time τ associated with any quasibound, or metastable, level characterized by a quasibound energy E.[4] We also constrain our study to structures in which τ_S, the scattering time from an electron occupying the state E, obeys $\tau \ll \tau_S$. This condition implies that the resonant tunneling through the state E is going to be, when produced, fully coherent and that the corresponding wave function on both sides of the structure has a definite phase relationship. In the other limit, if $\tau \gg \tau_S$, the resonant tunneling is said to be incoherent, or sequential, since the wave function loses the memory phase by scattering processes and consequently the wave function on both sides is only partially correlated. Our interest in coherent times comes from the fact that coherent tunneling seems to be the dominating mechanism in the high-speed DBRTS's.[5]

In the last decade a number of papers have focused their interest on the study of time scales for coherent tunneling processes in different semiconductor structures. That study was initiated by the calculation of the lifetimes of Stark resonant levels confined in single quantum wells. The effective-mass theory is the framework mostly used by those calculations.[6–9] Other schemes like the tight-binding method[10,11] or the $\mathbf{k}\cdot\mathbf{p}$ theory[12] are employed when the inclusion of Γ-X mixing or band structure details are wanted. As regards the calculation of the lifetime of electrons quasiconfined in DBRTS's, the effective-mass approach together with transmission coefficient analysis or the phase-shift method have been the procedures usually employed.[13,14] Recently, some of us have introduced the stabilization method brought from quantum chemistry, to evaluate in a unified way the total lifetime as well as the "left-hand" and "right-hand" decay rates $1/\tau_{r,l}$ for the trapped electron by using a Breit-Wigner generalization of the Lorentzian form of resonant transmision.[15]

A point to be stressed is that all the above-mentioned calculations use a model potential to avoid the cumbersome evaluation of the Hartree potential created by the electrons existing in the emitter and collector electrodes, and by the charge occasionally built up inside the quantum well (QW). One of the purposes of this work is to carry out such a calculation to establish how the doping profile affects the lifetime of the quasiconfined electrons and, therefore, to give the magnitude of the error produced when those model potentials are employed. Our goal is accomplished by performing the following steps: first, in Sec. II we obtain the self-consistent potential at a given voltage for the chosen doping profile by simultaneously solving the Schrödinger and Poisson equations, and second, in Sec. III we get the total tunneling time as well as its components by using the stabilization method. As regards the doping configuration we have investigated two cases; one in which the dopants are uniformly dis-

tributed, and another for which the dopant density is position dependent. This choice is motivated by the fact that they produce two limiting cases regarding the electronic configuration in the emitter; one in which the electrons in the emitter are fully three dimensional in the whole range of applied voltages (uniform-doping case), and another in which an accumulation layer appears in the emitter above a certain critical voltage and, consequently, a number of electrons have a two-dimensional (2D) character (gradually doped case). A comparison with the tunneling times obtained with a model potential is also given.

Another topic treated in this paper (Sec. IV) is the amount of charge accumulated in the emitter when the doping profile allows the existence of a quasi-two-dimensional level. We analyze the charge buildup in that level and in the QW level under forward and reverse applied bias in an asymmetric DBRTS. The different behavior between both situations has been measured and is qualitatively well understood in the literature. Nevertheless, to our knowledge there is no quantitative evaluation of such differences with the level of sophistication included here. Finally, we also give a phenomenological model to obtain the bistability region of our DBRTS.

II. THE SELF-CONSISTENT POTENTIAL PROFILE

The idealized band-edge potential profile experienced by an electron in a typical DBRTS built up with III-V semiconductors is shown in Fig. 1. The potential barriers V_0 are related to the alignment of the conduction bands between the epitaxially deposited layers at the Γ point of the Brillouin zone ($V_0 = \Delta E_c$). We transform the initially three-dimensional problem to a one-dimensional effective-mass equation by using an envelope-function approximation.[16] The envelope function $\psi_i(z)$ with energy E_i is the solution of the Schrödinger equation

$$-\frac{\hbar^2}{2m^*}\frac{d^2\psi_i(z)}{dz^2} + V(z)\psi_i(z) = E\psi_i(z) , \tag{1}$$

$$V(z) = -e\phi(z) + \Delta E_c(z) , \tag{2}$$

and the Poisson equation

$$\epsilon_0 k \frac{d^2\phi_i(z)}{dz^2} = e[n(z) - N_D(z)] , \tag{3}$$

where $n(z)$ is the electronic charge density, m^* is the effective mass of electrons, $\phi(z)$ is the electrostatic potential, E_i the bottom energy of the ith subband, $\epsilon_0 k$ the dielectric constant, and $N_D(z)$ the impurity charge density.

For simplicity, both m^* and $\epsilon_0 k$ are assumed to be constant in the whole system. Also, we have not considered any exchange-correlation term in Eq. (2) because it produces just minor effects on the properties of the DBRTS studied in the present work.[17,18]

Equation (1) is solved by setting the potential problem in between two infinite barriers. Therefore, the corresponding wave functions are subjected to the boundary condition $\psi_i(z) = 0$ at $z = 0$ and $z = L_1 + b_1 + w + b_2 + L_2 \equiv L$. This procedure will be justified in Sec. III. We numerically solve the given problem by expanding $\psi_i(z)$ in a linear combination of cubic B splines[19]

$$\psi_i(z) = \sum_j c_{ij} B_j(z) . \tag{4}$$

Using this localized basis the boundary condition is automatically obeyed by putting the $B_i(z)$ in the space just in between the two infinite barriers. Now, we place the expansion (4) in Eq. (1) and we arrive at the following general eigenvalue problem in matrix form:

$$(\mathbf{H} - E\mathbf{S})\mathbf{c} = 0, \tag{5}$$

where the matrix elements of the Hamiltonian $\mathbf{H}$ and the overlapping matrix $\mathbf{S}$ are

$$H_{ij} = \int_0^L B_i(z)\left(-\frac{1}{2m^*}\frac{d^2}{dz^2} + V(z)\right)B_j(z)dz , \tag{6}$$

$$S_{ij} = \int_0^L B_i(z)B_j(z)dz , \tag{7}$$

and the one-column matrix $\mathbf{c}$ gives the eigenfunctions.

Notice that the calculation is variational. Therefore we have to define in the space accessible to the wave function a sufficient number of B splines in order to make the calculated energy values converge. Furthermore, in order to obtain a good description of the wave function and its derivative along the whole structure, we have to put additional localized wave functions close to the regions where

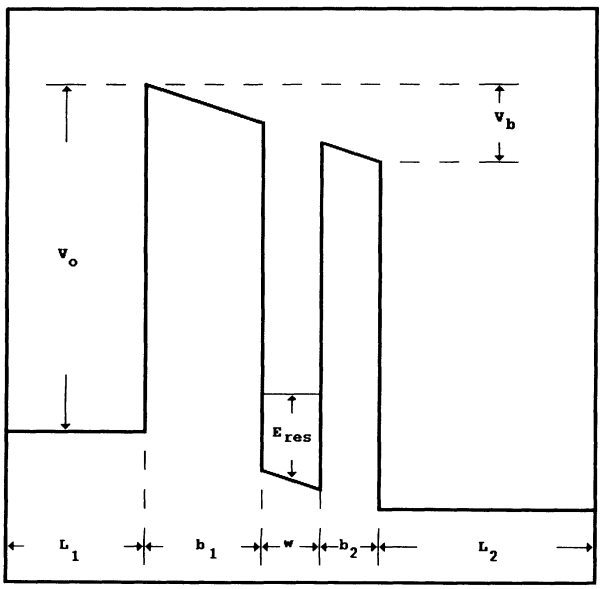

FIG. 1. Idealized flat-band potential energy profile for a double-barrier resonant-tunneling structure under an applied bias. The potential is not consistent with the charge distribution in the device. This arrangement of the barriers defines the forward bias configuration.

the potential is abrupt. A typical calculation is carried out by using a B spline every 20 Å, and four additional splines are put on both sides of the step potential, separated by 1×10^{-3} Å.

The electronic charge density is given by

$$n(z) = \sum_i N_i \psi_i^2(z), \tag{8}$$

where $\psi_i(z)$ is obtained from Eq. (4) and N_i is the number of electrons per unit area in subband i, given by

$$N_i = \frac{m^* k_B T}{\pi \hbar^2} \ln\left[1 + \exp\frac{(E_F - E_i)}{k_B T}\right], \tag{9}$$

$$N_i = \frac{m^*}{\pi \hbar^2}(E_F - E_i) \qquad \text{at } T = 0 \text{ K} .$$

The calculation is done mainly for the degenerate case by setting the temperature (T) to 0 K.

For an initial potential $V_{\text{in}}(z)$ (see for example the one in Fig. 1, where an initial bias V_b is defined) the solution of Eq. (5) gives the eigenvalues E_i and their corresponding eigenfunctions. The self-consistent process begins by filling those calculated levels up to a certain Fermi level. As regards this we have to distinguish two different situations.

(i) *Zero applied bias ($V_b = 0$).* In this case there is a unique Fermi level covering the whole structure, and it can be iteratively calculated by imposing the charge neutrality condition

$$\int_0^L n(z)dz = \frac{m^*}{\pi \hbar^2} \sum_i (E_F - E_i) = \int_0^L N_D(z)dz \ , \tag{10}$$

where the charge density has been obtained from Eqs. (4) and (5):

$$n(z) = \frac{m^*}{\pi \hbar^2} \sum_i (E_F - E_i)|\psi_i(z)|^2 \ . \tag{11}$$

(ii) *Nonzero applied bias ($V_b \neq 0$).* For this case we first classify the electronic levels E_i according to their spatial localization in the structure. Thus, we calculate the average positions $\langle z \rangle_i$ of the eigenstates with energies E_i,

$$\langle z \rangle_i = \int_0^L z|\psi_i(z)|^2 dz \ , \tag{12}$$

and separate them into emitter states E_i^e, collector states E_i^c, and QW states E_i^w. Afterwards, we define two different Fermi levels; one associated with the emitter, E_F^e, and another associated with the collector, E_F^c. Local charge neutrality conditions are separately imposed at each electrode to obtain the corresponding levels

$$\frac{m^*}{\pi \hbar^2} \sum_i (E_F^e - E_i^e) = \int_0^{L_1} N_D(z)dz \ , \tag{13}$$

$$\frac{m^*}{\pi \hbar^2} \sum_i (E_F^c - E_i^c) = \int_{L-L_2}^{L} N_D(z)dz \ , \tag{14}$$

and they define the final bias by $E_F^e = V_b + E_F^c$. In principle, we would define another local Fermi level associated with the QW region to take into account the occupation of its quasiconfined levels. We have simplified the calculation by including the QW level (or levels) either in the emitter side or in the collector side using an *ad hoc* procedure that will be justified in Sec. IV. Now, the total charge density $n(z)$ is

$$n(z) = \frac{m^*}{\pi \hbar^2} \sum_i (E_F^e - E_i^e)|\psi_i^e(z)|^2 + \frac{m^*}{\pi \hbar^2} \sum_i (E_F^c - E_i^c)|\psi_i^c(z)|^2 \ . \tag{15}$$

Once the Fermi level(s) is (are) defined and the corresponding charge density $n(z)$ is calculated a new total potential $V_{\text{out}}(z)$ is obtained after the resolution of the Poisson equation (3). The procedure explained up to now can be considered as the first step of a standard iterative procedure,[20] which finally gives the consistent potential. In particular, we control the convergence of the nth iteration using the parameter

$$\sigma_n = \sqrt{\frac{\sum_{k=1}^{N} |V_{\text{out}}^{(n)}(z_k) - V_{\text{in}}^{(n)}(z_k)|^2}{N(N+1)}} \ , \tag{16}$$

where N is the number of divisions, z_k, performed in the z axis ($N \approx 400$). A good convergence is obtained when $\sigma \approx 1$ or lower.

The theory so established is termed a "zero current" theory in the sense that no current is allowed to flow in establishing the self-consistent potential. Nevertheless, this level of sophistication has been proved to yield useful results even for devices with nonzero current.[21]

The generic epitaxial structure of all the systems studied in this paper is given in the table below:

Emitter contact	(In, Ga)As n type
Spacer layer (w_{sp})	(In, Ga)As intrinsic
Tunnel barrier (b_1)	(Al, In)As intrinsic
Quantum well (w)	(In, Ga)As intrinsic
Tunnel barrier (b_2)	(Al, In)As intrinsic
Spacer layer (w_{sp})	(In, Ga)As intrinsic
Collector contact	(In, Ga)As n type

with parameters $b_1 = 70$ Å, $w = 60$ Å, $b_2 = 40$ Å. We particularly study a $Ga_{0.47}In_{0.53}As$-$Al_{0.48}In_{0.52}As$ structure with a uniform effective mass $m^* = 0.041$, and a conduction-band-gap discontinuity $V_0 = 500$ meV.[22] Although we have neglected nonparabolicity effects and effective-mass differences between barriers and well, we do not expect any differences with the full calculation as has been demonstrated previously.[23]

We consider two structures with different spacer layer width w_{sp} and different doping concentrations $N_D(z)$ on the contact layers symmetrically distributed with respect to the barriers. The studied structures are the following.

(i) The uniform-doping structure with

$$w_{\text{sp}} = 50 \text{ Å}$$

and for the left electrode

$$N_D(z) = N_D = \text{const} = 2 \times 10^{18}\ \text{cm}^{-3} \text{ if } 0 \le z \le 1000\ \text{Å} . \quad (17)$$

(ii) The gradual-doping structure with

$w_{sp} = 250$ Å

and for the left electrode

$$N_D(z) = \begin{cases} N_D & \text{if } 0 \le z \le 500\ \text{Å} , \\ N_D - \frac{N_D - N_{D1}}{500}(z - 500) & \text{if } 500\ \text{Å} \le z \le 1000\ \text{Å} , \end{cases} \quad (18)$$

with $N_D = 2 \times 10^{18}$ cm^{-3} and $N_{D1} = 2 \times 10^{16}$ cm^{-3}. Some typical potential profiles obtained consistently for zero and nonzero applied bias are shown in Figs. 2 and 3, respectively.

We have compared the results obtained for these consistent profiles with the ones from a calculation in which the potential profile is analytically described by

$$V(z) = \begin{cases} 0 & \text{if } 0 \le z < L_1 , \\ V_0 - (z - L_1)F & \text{if } L_1 \le z < L_1 + b_1 , \\ -(z - L_1)F & \text{if } L_1 + b_1 \le z \le L_1 + b_1 + w , \\ V_0 - (z - L_1)F & \text{if } L_1 + b_1 + w \le z \le L_1 + b_1 + w + b_2 , \\ -V_b & \text{if } L_1 + b_1 + w + b_2 \le z \le L_1 + b_1 + w + b_2 + L_2 , \end{cases} \quad (19)$$

where F is the electric field along the z direction, which is related to the applied bias V_b by $F = V_b/(b_1 + w + b_2)$. This potential is plotted in Fig. 1. No consistency between the distribution of charge and potential is required in this case.

III. CALCULATION OF THE TUNNELING TIMES: THE STABILIZATION METHOD

The stabilization method (SM) was introduced in quantum chemistry as a general procedure to detect resonances in chemical reactions involving electron-atom or electron-molecule scattering.[24–26] The properties and pitfalls of this method have been recently reviewed by Riera[27] using a unified approach. In the field of solid state, some of us[8,15] have applied the SM to calculate the lifetimes of resonances in low-dimensional systems. In a few words, the basic idea behind this method consists of discretizing the continuum with which the resonance is interacting by setting the potential problem in between two infinite barriers. Afterwards, the behavior of the resulting eigenvalues as a function of the barrier separation is plotted in a graph. This graph is called the stabilization graph (SG) of the resonance and presents a characteristic pattern of avoided crossings between stable eigenvalues, which correspond to levels representing resonances, and unstable eigenvalues, related to the discretized continuum levels. For example, Fig. 4 shows a typical SG obtained for the double-barrier structure described in Fig. 1. In this particular case, the energy eigenvalues of Eq. (1) have been represented as a function of the distance L_2, the separation between the infinite right barrier and the left barrier of the QW. Now, from a graph like this it is possible to obtain the resonance energies as well as their lifetimes. With respect to this calculation, the structures analyzed in this work present different properties, regarding the characteristics of their resonances, that cause us to treat them separately in two cases which we explain in what follows.

A. Case I: One interacting resonance with the continuum

For this case the resonance under study must be isolated in the sense that it does not interact with any other resonance localized either inside or outside the QW. We have this situation for the uniformly doped structure, Eq. (17), and for the analytical potential, Eq. (19). We find two resonances associated with the QW, but they are

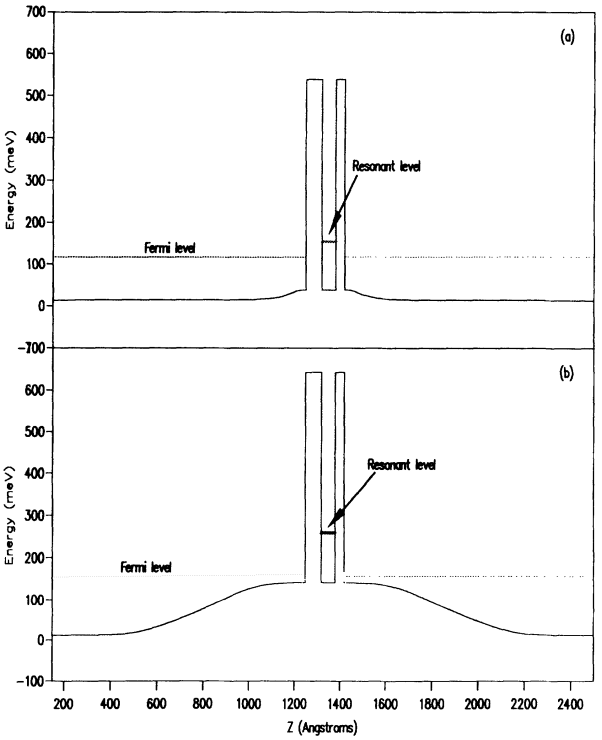

FIG. 2. Self-consistent potential energy profiles at zero voltage for a uniformly doped (a) and gradually doped (b) double-barrier structure.

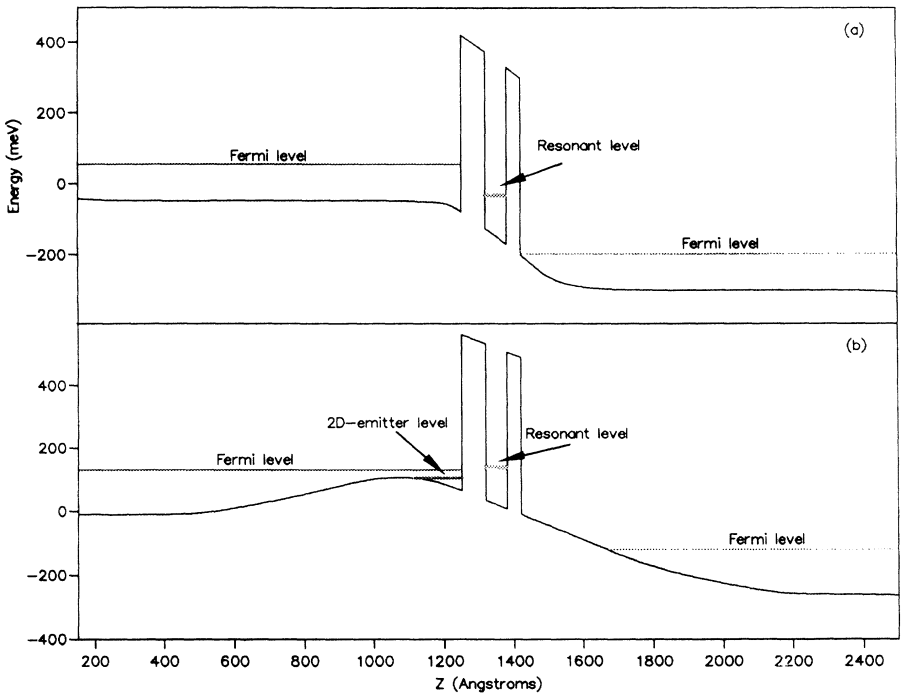

FIG. 3. Self-consistent potential energy profiles at $V_b \neq 0$ meV voltage for a uniformly doped (a), and gradually doped (b) double-barrier heterostructure.

well separated in energy and, therefore, can be treated separately.

The energy of one quasiconfined level, $E_{\rm res}$, as well as its lifetime can be obtained directly from the SG following the procedure below. We select two energy curves $E_1^{\rm SG}$,$E_2^{\rm SG}$ with an avoided crossing in the SG. They can be considered as solutions of a 2×2 secular problem:

$$\begin{vmatrix} H_{11} - E & V \\ V & H_{22} - E \end{vmatrix} = 0$$

whose solution is

$$E_{1,2} = \tfrac{1}{2}[H_{11} + H_{22} \pm \sqrt{(H_{11} - H_{22})^2 + 4V^2}] \quad (20)$$

with $H_{11} = E_{\rm res}$ and $H_{22} = E_c \sim 1/\mathcal{L}^2$ being the "uncoupled" states and V their interaction. This interaction is assumed to be localized near $\mathcal{L} = L_c$ (the crossing point).

To determine L_c we tabulate the function $R(\mathcal{L}) = \frac{1}{2}(E_1^{\rm SG} - E_2^{\rm SG})$ and find its minimum. Therefore at L_c

$$E_{1,2} = \tfrac{1}{2}(E_1 + E_2) \pm V \equiv \epsilon \pm V, \quad (21)$$

where $V = V(L_c) = \frac{1}{2}(E_1^{\rm SG} - E_2^{\rm SG})_{\rm minimum}$. The energy of the resonance can be calculated, with good approximation, as $E_{\rm res} = \epsilon$ (Refs. 8, 27).

As regards the resonance width Γ, it is calculated by using the standard golden-rule-type formula:[28]

$$\Gamma = 2\pi\rho(E)V^2 \ , \quad (22)$$

where $\rho(E)$ is the density of the "continuum" states. If E_n is the discretized continuum eigenvalue interacting with the stable one, the following is a good approximation for $\rho(E)$:

$$\rho(E) = \frac{2}{E_{n+1} - E_{n-1}} \ . \quad (23)$$

This formula is applicable if neither E_{n+1} nor E_{n-1} is contaminated by other stable eigenvalues.

Finally, to calculate the resonance lifetime, we employ the formula

$$\tau = \frac{\hbar}{\Gamma} \ , \quad (24)$$

which has been shown to be valid for heterostructures in which a single type of Bloch state is assumed.[29]

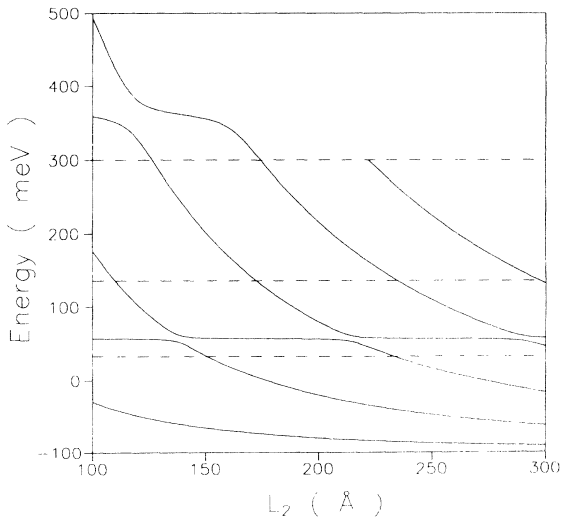

FIG. 4. Stabilization graph of the two quasibound states allowed in a DBRTS based on (Ga,In)As/(Al,In)As. The eigenvalues of Eq. (1) are represented versus the separation L_2 between the right barrier and the infinite barrier put in the collector side. The dashed lines correspond to energy levels confined on the left side of the structure.

The above-described procedure can be applied to any SG, independently of the variational distance $\mathcal{L}$ (L_1 or L_2) employed to get the graph. Of course, the physical meaning of the time obtained from a SG depends on the distance (L_1 or L_2) used in the mentioned SG because the continuum interacting with the resonance is different. Thus (i) by using the distance L_1 to the left-hand infinite barrier we obtain the left-hand tunneling time τ_l, and (ii) by using the distance L_2 to the right-hand infinite barrier (see Fig. 4) we obtain the right-tunneling time τ_r.

All the times are calculated in the complete coherent limit. Therefore the total elastic width Γ_t is related to the partial widths $\Gamma_{l,r}$ by $\Gamma_t = \Gamma_l + \Gamma_r$,[30] and consequently the total lifetime τ_t is given by

$$\frac{1}{\tau_t} = \frac{1}{\tau_l} + \frac{1}{\tau_r} . \tag{25}$$

The above-explained method has been applied with success to model asymmetric DBRTS's,[15] and it has been demonstrated that it gives identical results to the transmission coefficient method, regarding the total decay time.

B. Case II: Two interacting resonances with the continuum

The case of two resonances interacting with each other and, at the same time, interacting with a single continuum has scarcely been treated in the literature for the stabilization method. In our work, this situation appears for the gradually doped structure when the band bending in the emitter region at high voltages produces an accumulation layer where a two-dimensional (2D) state is quasiconfined. This accumulation layer has been experimentally detected,[31,32] and also theoretically analyzed.[33] From the theoretical point of view an analytical treatment has been performed for the particular case in which the level in the accumulation layer has a very long escape time τ. In what follows we analyze a more probable case, that in which the 2D level in the accumulation layer has a very short tunneling time to escape to the emitter side. This situation exists when that level is placed close to the top of the band bending. Nevertheless, the computational method here introduced can be applied to any case with independence of the degree of localizaton regarding the 2D emitter level, and it allows the calculation of all the tunneling times involved in the process: not only the times associated with the accumulation level but the ones associated with the QW level as well.

A typical SG of the avoided-crossing region of two resonances interacting with a level of the continuum is plotted in Fig. 5. The interacting terms as well as the resonance energies are obtained from this graph following the general ideas introduced in part A of this section.

Now, we consider that the three energy curves (for example, the ones shown in Fig. 5) are the solution of the following 3×3 secular problem:

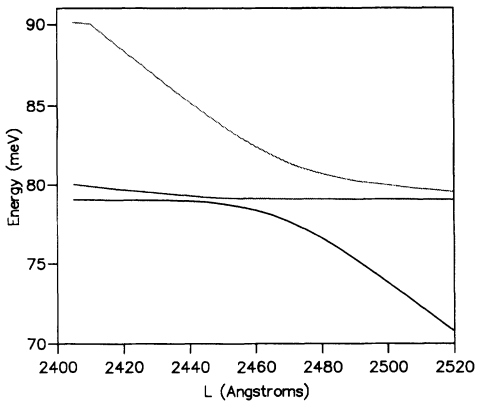

FIG. 5. Stabilization graph showing the case of the two resonances interacting with a *continuum* level (see Sec. III B).

$$\begin{vmatrix} H_{11}-E & 0 & V_1 \\ 0 & H_{22}-E & V_2 \\ V_1 & V_2 & H_{33}-E \end{vmatrix} = 0 , \tag{26}$$

where $H_{11} = E_{\mathrm{res},1} = C_1$ and $H_{22} = E_{\mathrm{res},2} = C_2$ are the two separate resonances interacting with the discretized continuum level $H_{33} = E_c = C_3 - C_4 L$, with their interacting parameters with the continuum $V_1 = C_5$ and $V_2 = C_6$. A standard procedure[34] gives the solutions $E_1(L)$, $E_2(L)$, and $E_3(L)$ which are functions of the six constants C_i introduced. These constants are obtained for a given SG by fitting the three generated curves to those from the SG. Numerically, the problem is reduced to minimizing the functional

$$\mathcal{F} = \sum_{j=1}^{M} \sum_{i=1}^{3} |E_i(L_j) - E_i^{\mathrm{SG}}(L_j)|^2 , \tag{27}$$

where E_i^{SG} are the SG energies and M is the number of points used for the fitting ($M \approx 20$).

The above-explained procedure presents the more general case. In practice, most of the calculation can be simplified to minimizing the functional with just two constants, the ones associated with V_1 and V_2, because the others are very well defined in the SG.

In Fig. 6(a) we show the calculated voltage dependence of the two resonance energies. The quasiconfined 2D emitter state begins to appear at about 40 mV and approaches the QW resonant level as the voltage increases. There is a region above 350 mV of approximately 75 mV wide in which both resonant levels interact and combine in order to form two mixing resonant levels (bonding and antibonding). Along this region the character of the initially nonmixed resonances gradually changes.[35]

Figure 6(b) shows the total decay time of each quasiconfined level as a function of voltage. The 2D emitter level has short lifetimes because its energy is close to the top of the band bending; therefore it has a very high probability of escaping to the emitter side. The region of interaction is clearly separated in the figure, and the lifetimes in this region are assigned to either the bonding (B) or the antibonding (A) combination without men-

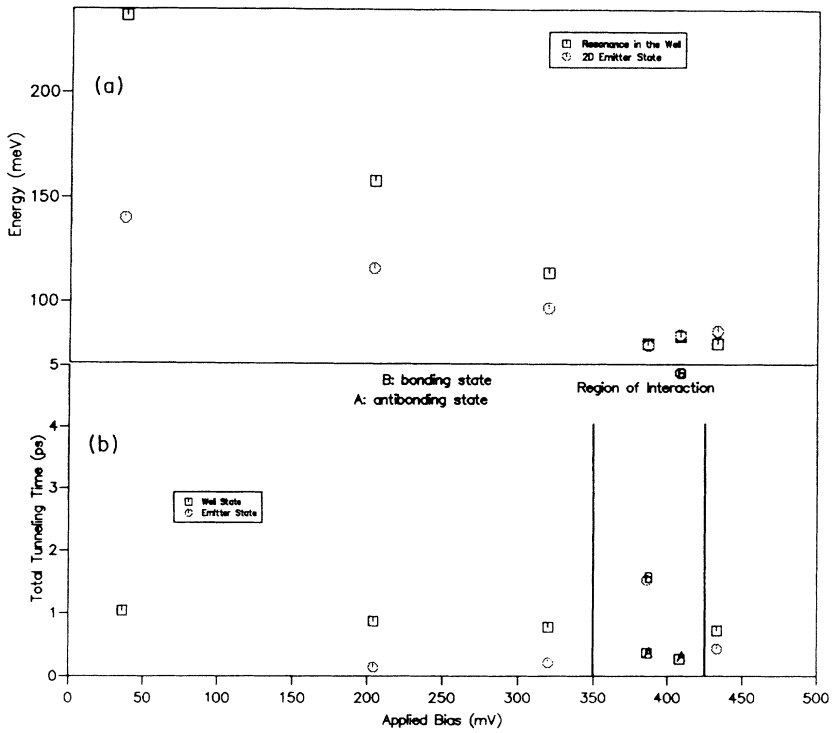

FIG. 6. Behavior of the 2D emitter and well resonant energy levels (a) and their corresponding total lifetimes (b) as a function of voltage for the gradually doped structure. In the interaction region A and B denote the antibonding and bonding combinations.

tion of their main character. At this point, let us remark how the tunneling time of the 2D emitter level, initially very short, becomes comparable to that of the QW level in the interaction region due to the mixing. Similar behavior has been explained previously for the case of a 2D level with very long decay times[33] and for double quantum wells under an electric field.[35] As we will see in Sec. IV, this effect produces observable consequences on the behavior of the charge accumulated in both levels.

The wave-function-mixing effect is shown in Fig. 7 where we plot the bonding and antibonding wave functions at two different voltages, before and after the theoretical crossing voltage. Notice how for the lower voltage, $V_b = 407$ mV, the amplitude of the wave-function oscillations is higher in the emitter (QW) side for the bonding (antibonding) combination, denoting its prevailing emitter (QW) character. The opposite behavior occurs at the higher voltage, $V_b = 420$ mV.

C. Results and discussion

The right- and left-hand tunneling times obtained for the first QW resonance in the structures under study are shown in Fig. 8 for forward bias. The total decay times (not shown) are practically the same as the right-hand

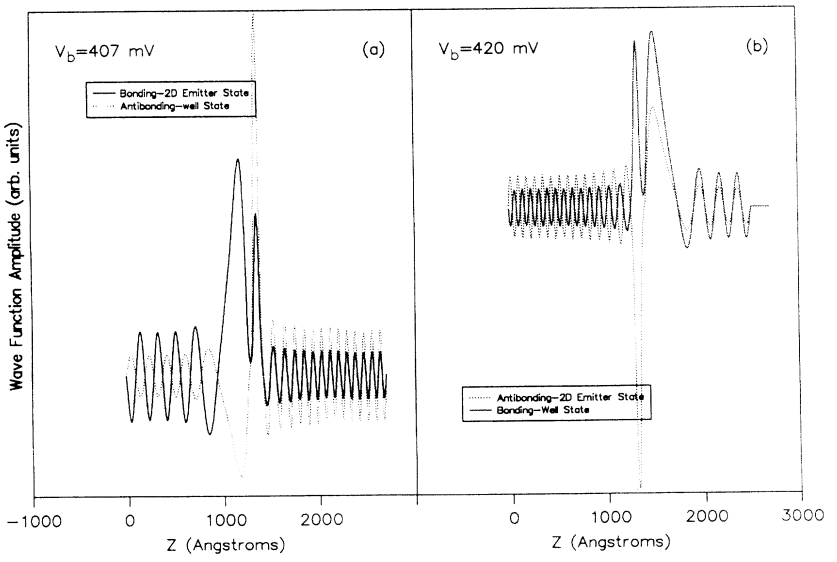

FIG. 7. Electronic wave functions of the bonding and antibonding combinations of the two interacting levels quasiconfined in the gradually doped structure before (a) and after (b) the maximum-mixing voltage.

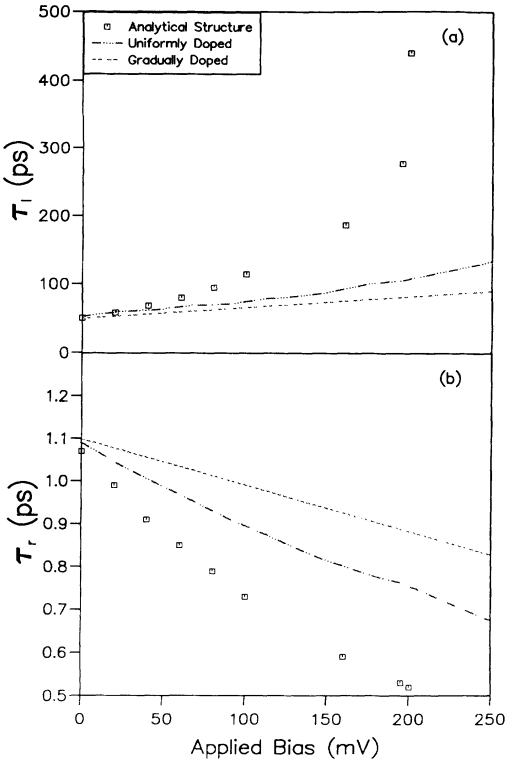

FIG. 8. Comparison between the left- (a) and right-hand (b) tunneling times (τ_l and τ_r, respectively) calculated for the three heterostructures analyzed in this work under forward bias.

tunneling times [see Eq. (25)]. For the gradual doping case we plot in Fig. 9 the same magnitudes but for a wider range of voltages. This case presents a special behavior for the range of voltage for which the interaction between the two quasiconfined levels (the 2D emitter level and the QW level) takes place. The mixing of the states produces τ_r (τ_l) longer (shorter) than the expected one. Outside the above-mentioned range of voltages the

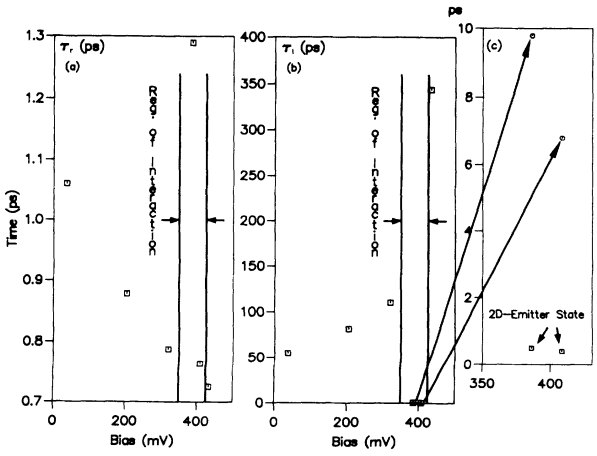

FIG. 9. Comparison between the right- (a) and left-hand (b) tunneling times (τ_r and τ_l, respectively) calculated for the gradually doped structure in the whole range of analyzed voltages for the forward bias configuration.

analytical potential always underestimates τ_r and overestimates τ_l. Moreover, the gradually doped structure always gives the shortest τ_l and the longest τ_r times. Also, the differences between the times calculated for the different models increase with voltage. At this point one has to remark that the main effect of the charge distribution on the tunneling times is to produce a smoothing of their voltage dependence. As regards the influence of this calculated behavior on the current-voltage (I-V) characteristics of the structure, in a heterostructure diode the current contributed by the coherent resonance is generally proportional to $1/(\tau_l+\tau_r)$ (Ref. 36; see also Sec. IV) and this dependence implies that the gradually doped structure will show the highest currents. This simple effect seems to explain why the highest peak-valley ratios are obtained in DBRTS's with strong band bending.[31] Of course, this analysis should be completed with a careful calculation of the tunneling currents, which will be the purpose of a separate work.

On the other hand, the critical voltage at which the escape probability to the left side is zero (i.e., $\tau_l = \infty$), which roughly corresponds to the region of negative differential resistance in the I-V characteristics, shifts to higher voltage when the potential profile dependence upon the charge distribution is taken into account, and this shift gets larger as the band bending increases. This effect will be shown in the I-V curve of the structure as a shift to higher voltage of the negative differential resistance region, as has been previously calculated.[37]

IV. EFFECTS OF CHARGE BUILDUP

Charge buildup inside the QW produces bistable regions in the current-voltage response in a DBRTS.[38–42] In order to allow the electrons to accumulate, the collector barrier should have a certain thickness. On the other hand, it has been proposed that the peak-valley ratio, which is a measure of the quality of the DBRTS for device applications, increases when an accumulation layer is produced in the emitter side by controlling the doping profile.[31] An accumulation layer of such characteristics appears in our gradually doped structure [Eq. (18)] as has been explained above [see Fig. 2(b)]. In what follows we analyze the charge buildup in that layer as well as the one accumulated inside the QW. The procedure to obtain these charges is simple; we have to integrate the corresponding charge density $n(z)$ over the accumulation region or the QW region.

In principle, the calculation of $n(z)$ implies previous knowledge of the position dependence along the structure of the Fermi level, $E_F(z)$, which is a difficult task.[41,42] Instead of that we have used the properties associated with the structure under study to elaborate a simple model in which just two Fermi levels have to be defined: at the emitter and collector electrodes, respectively [Eqs. (13) and (14)]. So at a given bias $n(z)$ [Eq. (15)] involves just the occupation of emitter and collector states. As to the occupation of the accumulation level at the emitter or the QW levels, several comments are introduced below.

As regards the accumulation level, we consider it in thermodynamic equilibrium with the emitter. The rea-

son for that is its very short escape time to the emitter side, τ_l, which easily allows its occupation by diffusion of carriers coming from the emitter. Therefore we include it in Eq. (15) as a true emitter state.

In relation to the QW level its occupation, $F_w(E)$, can be modeled by means of the sequential approach.[43] In this approach it is assumed that the electron first tunnels into the well and afterwards escapes by tunneling through the collector barrier. Following similar arguments by Weil and Vinter,[44] the steady-state population of the well can be found by balancing the incoming and outgoing fluxes. Thus, for the case in which the collector Fermi level is below the QW energy level Eq. (11) of Ref. 44 gives

$$F_w(E) = \frac{\tau_r}{\tau_l + \tau_r} F_l(E) \ . \tag{28}$$

A more general expression can be formulated in order to consider the possibility of having the collector Fermi level above the QW energy level. For this case,

$$F_w(E) = \frac{\tau_r}{\tau_l + \tau_r} F_l(E) + \frac{\tau_l}{\tau_l + \tau_r} F_r(E) \ , \tag{29}$$

where $F_{l,w,r}(E) = \sum_k \sum_\sigma f_{l,w,r}(E,k,\sigma)$ (where f is the electron distribution function). The tunneling current can formulated as

$$j(E) = \frac{F_l(E) - F_r(E)}{\tau_l + \tau_r} \ . \tag{30}$$

Now, Eq. (29) together with the values of $\tau_{l,r}$ gives us the method for assigning the character of the QW state. For the asymmetric structure considered in this work, we can distinguish two different cases according to the relative position of the barriers with respect to the electrodes.

(i) *Forward bias.* In this case, the emitter barrier is the thick one and, except for voltages for which the 2D emitter and the QW levels interact, we find (see Fig. 9) $\tau_r \ll \tau_l$. Then Eq. (29) reduces to

$$F_w(E) \approx F_r(E) \tag{31}$$

and consequently the QW level must be added in Eqs. (14) and (15) as a true collector level. This condition implies that the QW level is going to be empty for all voltages because the energy of the QW level is always above the collector Fermi level.

For the region of voltages for which the mixing of the 2D emitter state and the QW state is produced, there are two states with a partial QW character. These states have $\tau_r \approx \tau_l$. One of these states is filled as an emitter state and the other is occupied as a collector state. This criterion can be justified with Eq. (29). With $\tau_r \approx \tau_l$, we have

$$F_w(E) \approx \frac{F_l(E) + F_r(E)}{2} \ . \tag{32}$$

Then, for this case, a small quantity of charge is accumulated inside the QW due to the wave-function mixing of the 2D emitter and the QW levels.

(ii) *Reverse bias.* Now the emitter barrier is the thin one. For this case $\tau_l \ll \tau_r$ and then Eq. (29) reduces to

$$F_w(E) \approx F_l(E) \ . \tag{33}$$

Therefore the QW level can be considered as an emitter level and can be added as a true emitter level in Eqs. (13)–(15).

The results obtained for the buildup of 2D charge density in the accumulation layer, n_s, and for the charge density accumulated in the QW, n_w, are plotted in Figs. 10 and 11, respectively, in which forward and reverse biases are considered separately. From the experimental point of view, the 2D charge density can be determined from the periodicity of the current oscillations when a magnetic field $\mathbf{B}$ is applied perpendicularly to the interfaces, $\mathbf{B} \parallel \mathbf{J}$.[45,46] For the sake of comparison, we show in Fig. 12 the corresponding charge experimentally measured in an accumulation layer of an $Al_xGa_{1-x}As/GaAs$-based DBRTS.[47] Notice the very good general agreement with our calculation. There is even a quantitative agreement that should be considered as fortuitous, because we consider different structures.

The observed behavior is understood in the following terms.

(a) For the case of forward bias, the collector barrier is the thin one and, therefore, the current is controlled just by the emitter barrier. In this case, the resonant QW level has a too short tunneling time τ_r to hold the electrons in the well. Then the charge density accumulated in the emitter increases as the voltage increases almost linearly. In this case, a small amount of charge is accumulated in the QW due to the above-mentioned wave-function mixing.

(b) For reverse bias, the collector barrier is the thick one. Therefore it confines the electrons in the emitter as well as in the QW level. The observed saturation for n_s corresponds to the thermalization of the 2D electronic

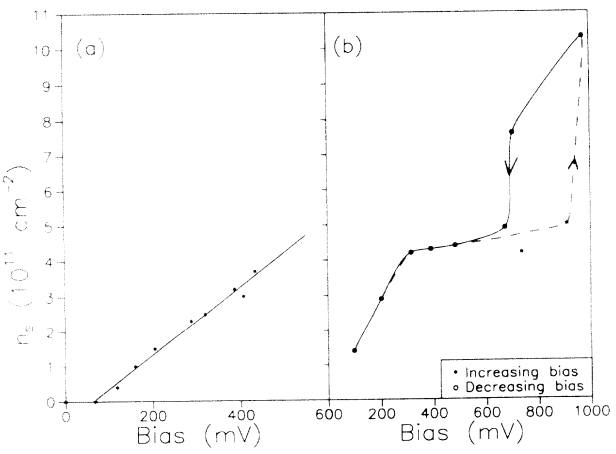

FIG. 10. Two-dimensional charge density built up in the accumulation layer, n_s, at the emitter for the gradually doped structure as a function of voltage for forward (a) and reverse (b) bias configurations. For reverse bias a bistable region appears due to the possibility of having the QW level charged (increasing bias) or empty (decreasing bias). Lines are guides for the eyes.

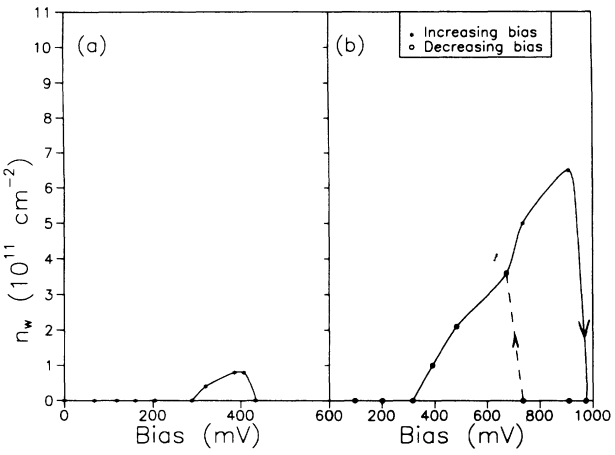

FIG. 11. Two-dimensional charge density accumulated in the QW, n_w, for the gradually doped structure for the forward (a) and the reverse (b) bias configurations. For the reverse bias configuration, a bistable region appears. Lines are guides for the eyes.

gas in the emitter with the electrons confined in the QW due to their wave-function mixing. Our calculation also predicts a bistable region in the n_s-V curve that appears at the end of the saturation region [between 650 and 850 mV in Fig. 10(b)]. This bistable region correlates with the bistable region experimentally observed in the I-V curve.[32] The link between both bistable regions is easily understood from Eq. (30). For sufficiently high voltages the collector Fermi level is below the QW level, and then Eq. (30) can be simplified to

$$j(E) = \frac{F_l(E)}{\tau_l + \tau_r} . \tag{34}$$

For increasing bias, the QW level is included in $F_l(E)$; for decreasing bias, it is not included. These two possibilities give the two different values for n_s at a given voltage and, consequently, the two different solutions for $j(E)$, through Eq. (33). For the case of increasing bias, the range of saturation for n_s is enlarged due to the interaction between the QW and the 2D emitter levels (see Fig. 6). On the other hand, for the case of decreasing bias, the region of saturation is shorter because the QW level is empty (see Fig. 10). This behavior of n_s is correlated with that of the charge accumulated in the QW, n_w, that is plotted in Fig. 11. n_w increases in the range of saturation of n_s and behaves bistably in the same range as n_s.

To the best of our knowledge the bistable region in n_s-V characteristics has not been experimentally reported, probably due to the difficulty of assigning the 2D charge to the QW or to the emitter accumulation level for the critical range of voltage. For our structure we estimate a bistable region approximately 200 meV wide.

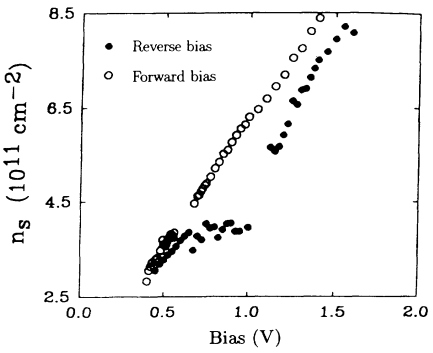

FIG. 12. Typical experimental results where the two-dimensional charge density n_s accumulated in the emitter is measured as a function of voltage for the two possible bias configurations. The data correspond to an asymmetric gradually doped $Al_xGa_{1-x}As/GaAs$-based double barrier and have been taken from Ref. 47.

V. SUMMARY

In conclusion, we have calculated in a unified way the two contributions to the total decay time of electrons confined in the quantum well of two different asymmetric double-barrier resonant-tunneling structures; one uniformly doped and the other gradually doped. In both cases the potentials were self-consistently calculated by simultaneously solving the Schrödinger and Poisson equations. Afterwards, the partial times were obtained by means of the stabilization method. The resulting times were compared with the ones obtained using the simplified potential normally considered for simulating these structures. As regards the forward bias configuration, the comparison indicates that the structure with larger band bending, the gradually doped one, gives the shorter (longer) tunneling times to escape to the emitter (collector) side, τ_l (τ_r). The model potential, without band bending, always underestimates τ_r and overestimates τ_l and differences increase with voltage.

For the gradually doped structure we have also investigated charging effects associated with the existence of an accumulation layer at the emitter electrode. Our results regarding the dependence on the voltage of the 2D charge buildup in that layer, n_s, at different bias configurations agree qualitatively with the experimental observation in similar structures. Also, we have shown that in these structures a bistable region in the I-V curve implies a bistable region in the n_s-V characteristics, which is predicted by our calculation but, to our knowledge, has not been experimentally detected yet.

ACKNOWLEDGMENTS

This work was partially supported by the Comisión Interministerial de Ciencia y Tecnología of Spain under Contract MAT 94-0727 and by the European Community under its Human Capital and Mobility program. We thank Dr. L. Cury and Dr. A. Nogaret for helpful discussions.

[1]E. H. Hauge and J. A. Støvneng, Rev. Mod. Phys. **61**, 917 (1989).
[2]A. P. Jauho, in *Hot Carriers in Semiconductor Nonostructures*, edited by J. Shah (Academic, New York, 1992), p. 121.
[3]R. Landauer and Th. Martin, Rev. Mod. Phys. **66**, 217 (1994).
[4]A. Galindo and P. Pascual, *Quantum Mechanics* (Springer-Verlag, Berlin, 1990).
[5]F. Capasso, K. Mohammed, and A. Y. Cho, IEEE J. Quantum Electron. **22**, 1853 (1986).
[6]E. J. Austin and M. Jaros, Phys. Rev. B **31**, 5569 (1985).
[7]E. J. Austin and M. Jaros, Appl. Phys. Lett. **47**, 274 (1985).
[8]F. Borondo and J. Sánchez-Dehesa, Phys. Rev. B **33**, 8758 (1986).
[9]D. Ahn and S. L. Chuang, Phys. Rev. B **34**, 9034 (1986).
[10]P. A. Schultz and C. E. T. Goncalvez da Silva, Phys. Rev. B **35**, 8126 (1987).
[11]L. Brey and C. Tejedor, Solid State Commun. **61**, 573 (1987).
[12]R. Lassnig, Solid State Commun. **61**, 577 (1987).
[13]T. B. Bahder, C. A. Morrison, and J. D. Bruno, Appl. Phys. Lett. **51**, 1089 (1987).
[14]J. P. Peng, H. Chen, and S.-X. Zhou, Phys. Rev. B **43**, 12 042 (1991).
[15]J. A. Porto, J. Sánchez-Dehesa, L. A. Cury, A. Nogaret, and J. C. Portal, J. Phys. Condens. Matter **6**, 887 (1994).
[16]G. Bastard, *Wave Mechanics Applied to Semiconductor Heterostructures* (Les Editions de Physique, Les Ulis, 1988).
[17]J. Zhang and W. Pötz, Phys. Rev. B **42**, 11 366 (1990).
[18]N. Zou, M. Willander, I. Linnerud, U. Hanke, K. A. Chao, and Y. M. Galperin, Phys. Rev. B **49**, 2193 (1994).
[19]C. de Boor, *A Practical Guide to Splines* (Springer, New York, 1978).
[20]T. Ando, A. B. Fowler, and F. Stern, Rev. Mod. Phys. **54**, 437 (1982).
[21]J. H. Luscombe, J. N. Randall, and A. M. Bouchard, Proc. IEEE **79**, 1117 (1991).
[22]R. People, K. W. Wecht, K. Alavi, and A. Y. Cho, Appl. Phys. Lett. **43**, 118 (1983).
[23]L. A. Cury and J. C. Portal, Phys. Rev. B **44**, 6224 (1991); L. A. Cury, Ph.D. thesis, INSA, Toulouse, 1992.
[24]E. Holøien and J. Midtal, J. Phys. B **3**, 592 (1970).
[25]H. S. Taylor, Adv. Chem. Phys. **18**, 91 (1970).
[26]A. U. Hazi and H. S. Taylor, Phys. Rev. A **1**, 1109 (1970).
[27]A. Riera, J. Phys. Chem. **97**, 1558 (1993).
[28]For a critical discussion of this point, see Sec. 2 of Ref. 27, and references therein.
[29]P. J. Price, Superlatt. Microstruct. **2**, 593 (1986).
[30]For a discussion of this point, see M. Büttiker, IBM J. Res. Dev. **32**, 63 (1988).
[31]J. S. Wu, C. P. Lee, C. Y. Chang, D. G. Liu, and D. C. Liou, J. Appl. Phys. **69**, 1122 (1991).
[32]L. A. Cury, D. K. Maude, F. Aristone, J. C. Portal, D. L. Sivco, A. Y. Cho, and G. Hill, Surf. Sci. **267**, 383 (1992).
[33]P. J. Price, Phys. Rev. B **45**, 9042 (1992).
[34]*Handbook of Mathematical Functions*, edited by M. Abramowitz and I. Stegun (Dover, New York, 1970).
[35]M. Wagner and H. Mizuta, Phys. Rev. B **48**, 14 393 (1993).
[36]P. J. Price, Phys. Rev. B **38**, 1994 (1988).
[37]M. Cahay, M. McLennan, S. Datta, and M. S. Lundstrom, Appl. Phys. Lett. **50**, 612 (1987).
[38]V. J. Goldman, D. C. Tsui, and J. E. Cunningham, Phys. Rev. Lett. **58**, 1257 (1987).
[39]F. W. Sheard and G. A. Toombs, Appl. Phys. Lett. **52**, 1228 (1988).
[40]J. F. Young, B. M. Wood, G. C. Ares, R. L. S. Devine, H. C. Liu, D. Landheer, M. Buchanan, A. J. Springthorpe, and P. Mandeville, Phys. Rev. Lett. **60**, 2085 (1988).
[41]J. O. Sofo and C. A. Balseiro, Phys. Rev. B **42**, 7292 (1990).
[42]P. Pernas, F. Flores, and E. Anda, Phys. Rev. B **47**, 4779 (1993).
[43]S. Luryi, Appl. Phys. Lett **47**, 490 (1985).
[44]T. Weil and B. Vinter, Appl. Phys. Lett. **50**, 1281 (1987).
[45]L. Eaves, E. S. Alves, M. Henini, O. H. Hughes, M. L. Leadbeater, C. A. Payling, F. W. Sheard, G. A. Toombs, A. Celeste, J. C. Portal, G. Hill, and M. A. Pate, in *High Magnetic Fields in Semiconductor Physics II*, edited by G. Landwehr (Springer-Verlag, Berlin, 1989).
[46]V. J. Goldman, B. Su, and J. E. Cunningham, in *Resonant Tunneling in Semiconductors*, edited by L. L. Chang, E. E. Méndez, and C. Tejedor (Plenum Press, New York, 1991), p. 431.
[47]A. Nogaret, Ph.D. thesis, INSA, Toulouse, 1994.